NUMERICAL SIMULATION OF 3-D SOBOLEV EQUATION VIA LOCAL MESHLESS METHOD

by

Imtiaz AHMAD[a*], Muhammad AHSAN[a], Abd Elmotaleb A. M. A. ELAMIN[b], Sayed ABDEL-KHALEK[c], and Mustafa INC[d,e*]

[a] Department of Mathematics, University of Swabi, Khyber Pakhtunkhwa, Pakistan
[b] Department of Mathematics, College of Science and Humanity,
Prince Sattam bin Abdulaziz University, Sulail, Saudi Arabia
[c] Department of Mathematics, College of Science, Taif University, Taif, Saudi Arabia
[d] Firat University, Science Faculty, Department of Mathematics, Elazig, Turkiye
[e] Department of Medical Research, China Medical University,Taichung, Taiwan

Original scientific paper
https://doi.org/10.2298/TSCI22S1457A

In this study, we use an effective meshless method to estimate the numerical solution of 3-D time-fractional Sobolev equation. The recommended meshless method is used for the spatial derivatives while the Liouville-Caputo derivative technique is utilized for the time derivative portion of the model equation. Accuracy of the method is assessed via error norms and comparison is made with the exact solution and other numerical methods given in more current literature, which demonstrated that the suggested strategy produces excellent performance and is more computationally efficient.

Key words*: local meshless method, Liouville-Caputo derivative, 3-D Sobolev equations, irregular domain*

Introduction

In a later decade, there was a lot of attention given to fractional PDE with time-fractional derivatives. It emerged to become a cutting-edge instrument for the more accurate description of numerous physical and technical processes. The FPDE contains the unknown multivariable function and its fractional partial derivatives. The FPDE are used to model problems with functions of several variables, to find solution of many physical models. Essential information about the fractional calculus can be found in [1]. We consider a class of 3-D Sobolev equations which are defined:

$$\frac{\partial^{\alpha} W(\bar{r},t)}{\partial t^{\alpha}} - \frac{\partial \nabla^2 W(\bar{r},t)}{\partial t} - \beta \nabla^2 W(\bar{r},t) + \gamma \nabla \left(W(\bar{r},t) \nabla W(\bar{r},t) \right) + \delta W(\bar{r},t) = F(\bar{r},t), \quad \bar{r} \in \Omega \subset \mathbb{R}^3,\ 0 < \alpha \leq 1,\ t > 0 \tag{1}$$

with the conditions

$$W(\bar{r},0) = W_0(\bar{r}), \quad W(\bar{r},t) = g_1(\bar{r},t), \quad \bar{r} \in \partial\Omega \tag{2}$$

* Corresponding author, e-mails: imtiazkakakhil@gmail.com, minc@firat.edu.tr

where ∇^2 and ∇ are the Laplacian Gradient operators, respectively, and β, γ, and δ is the known constants. Moreover, $\partial^\alpha/\partial t\alpha$ represent the Caputo derivative [2] for $0 < \alpha \leq 1$, for $W(r, t)$.

Practically in all areas of mathematics and physics, meshless approaches have lately been proven to be useful tools for solving diverse PDE models. The most popular of these are meshless approaches based on the radial basis function (RBF). Because of their meshless characteristics, these approaches are particularly well-liked by researchers. A variety of physical issues can be addressed using meshless approaches [3-6]. The most prominent drawbacks of meshless approaches are the dense ill-conditioned matrices and picking the ideal shape parameter value. To address these issues, researchers created the local meshless method, which is reliable and efficient in solving a variety of fractional and integer order PDE models [7, 8]. In comparison the global meshless version, these approaches yield sparse matrices that are well-conditioned and are less sensitive to shap parameter selection. These methods have recently undertaken testing in several applications [9-16].

The local meshless method (LMM) is included in this study to numerically simulate the time-fractional model (1). In addition, numerical examinations take into account both regular and irregular domains.

Local meshless scheme

In the proposed methodology, the derivatives of $W(\bar{\mathbf{r}}, t)$ are approximated at the centers $\bar{\mathbf{r}}_h$ by the neighborhood of $\bar{\mathbf{r}}_h$:

$$\{\bar{r}_{h1}, \bar{r}_{h2}, \bar{r}_{h3}, ..., \bar{r}_{hn_h}\} \subset \{\bar{r}_1, \bar{r}_2, \ldots, \bar{r}_{N^n}\}, \; n_h \ll N^n$$

where $h = 1, 2, ..., N^n$. In case of 1-D, 2-D, and 3-D case $\bar{\mathbf{r}} = x$, $\bar{\mathbf{r}} = (x, y)$, and $\bar{\mathbf{r}} = (x, y, z)$, respectively.

Procedure for 1-D case:

$$W^{(m)}(x_h) \approx \sum_{k=1}^{n_h} \lambda_k^{(m)} W(x_{hk}), \;\; h = 1, 2, \ldots, N \tag{3}$$

Substituting RBF $\psi||x - x_p||$ in eq. (3):

$$\psi^{(m)}(\| x_h - x_p \|) = \sum_{k=1}^{n_h} \lambda_{hk}^{(m)} \psi(\| x_{hk} - x_p \|), \;\; p = h_1, h_2, \ldots, hn_h \tag{4}$$

we get the equation:

$$\psi_{n_h}^{(m)} = \mathbf{A}_{n_h} \lambda_{n_h}^{(m)} \tag{5}$$

From eq. (5), we obtain:

$$\lambda_{n_h}^{(m)} = \mathbf{A}_{n_h}^{-1} \psi_{n_h}^{(m)} \tag{6}$$

eqs. (3) and (6) imply

$$W^{(m)}(x_h) = \left(\lambda_{n_h}^{(m)}\right)()^T \mathbf{W}_{n_h}$$

where

$$\mathbf{W}_{n_h} = \left[W(x_{h1}), W(x_{h2}), \ldots, W(x_{hn_h})\right]^T$$

The derivatives of $W(x, y, t)$ w.r.t. x and y can be found:

$$W_x^{(m)}(x_h, y_h) \approx \sum_{k=1}^{n_h} \gamma_k^{(m)} W(x_{hk}, y_{hk}), \quad h = 1, 2, \ldots, N^2$$

$$W_y^{(m)}(x_h, y_h) \approx \sum_{k=1}^{n_h} \eta_k^{(m)} W(x_{hk}, y_{hk}), \quad h = 1, 2, \ldots, N^2$$

For $\gamma_k^{(m)}$ and $\eta_k^{(m)}$ ($k = 1, 2, ..., n_h$), we get:

$$\gamma_{n_h}^{(m)} = \mathbf{A}_{n_h}^{-1} \boldsymbol{\Phi}_{n_h}^{(m)}$$

$$\eta_{n_h}^{(m)} = \mathbf{A}_{n_h}^{-1} \boldsymbol{\Phi}_{n_h}^{(m)}$$

Similar procedure can be adopted for 3-D case.

Time discretization

The Caputo derivative [2] is utilized for time-fractional derivative:

$$\frac{\partial^\alpha W(\bar{r}, t)}{\partial t^\alpha}$$

for $\alpha \in (0, 1)$:

$$\frac{\partial^\alpha W(\bar{r}, t)}{\partial t^\alpha} = \begin{cases} \dfrac{1}{\Gamma(1-\alpha)} \displaystyle\int_0^t \frac{\partial W(\bar{r}, \vartheta)}{\partial \vartheta} (t - \vartheta)^{-\alpha} \, d\vartheta, & 0 < \alpha < 1 \\ \dfrac{\partial W(\bar{r}, t)}{\partial t}, & \alpha = 1 \end{cases}$$

We can obtain the derivative term as follows, where $t_q = q\tau$, $q = 0, 1, 2, ..., Q$ and time step size $\Delta\tau$ in $[0, t]$:

$$\frac{\partial^\alpha W(\bar{r}, t_{q+1})}{\partial t^\alpha} = \frac{1}{\Gamma(1-\alpha)} \int_0^{t_{q+1}} \frac{\partial W(\bar{r}, \vartheta)}{\partial \vartheta} \left(t_{q+1} - \vartheta\right)^{-\alpha} \mathrm{d}\vartheta$$

$$\approx \frac{1}{\Gamma(1-\alpha)} \sum_{s=0}^{q} \int_{s\tau}^{(s+1)\tau} \frac{\partial W(\bar{r}, \vartheta_s)}{\partial \vartheta} \left(t_{s+1} - \vartheta\right)^{-\alpha} \mathrm{d}\vartheta$$

The term

$$\frac{\partial W(\bar{r}, \vartheta_s)}{\partial \vartheta}$$

can be approximated:

$$\frac{\partial W(\bar{r}, \vartheta_s)}{\partial \vartheta} = \frac{W(\bar{r}, \vartheta_{s+1}) - W(\bar{r}, \vartheta_s)}{\vartheta} + \mathcal{O}(\tau)$$

Then:

$$\frac{\partial^{\alpha} W(\bar{r},t_{q+1})}{\partial t^{\alpha}} \approx \frac{1}{\Gamma(1-\alpha)} \sum_{s=0}^{q} \frac{W(\bar{r},t_{s+1}) - W(\bar{r},t_s)}{\tau} \int_{s\tau}^{(s+1)\tau} \left(t_{s+1} - \vartheta\right)^{-\alpha} \mathrm{d}\vartheta$$

$$\begin{cases} \dfrac{\tau^{-\alpha}}{\Gamma(2-\alpha)}(W^{q+1} - W^{q}) + \dfrac{\tau^{-\alpha}}{\Gamma(2-\alpha)} \displaystyle\sum_{s=1}^{q} (W^{q+1-s} - W^{q-s})[(s+1)^{1-\alpha} - s^{1-\alpha}], & q \geq 1 \\ \dfrac{\tau^{-\alpha}}{\Gamma(2-\alpha)}(W^{1} - W^{0}), & q = 0 \end{cases}$$

Letting:

$$a_0 = \frac{\tau^{-\alpha}}{\Gamma(2-\alpha)} \text{ and } b_s = (s+1)^{1-\alpha} - s^{1-\alpha},\ s = 0,1,\ldots,q$$

we have:

$$\frac{\partial^{\alpha} W(\bar{r},t_{q+1})}{\partial t^{\alpha}} \approx \begin{cases} a_0(W^{q+1} - W^{q}) + a_0 \displaystyle\sum_{s=1}^{q} b_s (W^{q+1-s} - W^{q-s}), & q \geq 1 \\ a_0(W^{1} - W^{0}), & q = 0 \end{cases} \tag{7}$$

Numerical discussion

The proposed LMM is evaluated for its ability to accurately and efficiently approximate the solution of model eq. (1). One example is considered using scatted and uniform nodes with non-rectangular and rectangular domain. Throughout the paper, we have used IMQ RBF with shape parameter value $c = 15 \cdot 10^5$. The local stencil seven in the spatial domain [0, 4] are utilized unless mentioned explicitly. For accuracy measurement, we used the following error norms:

$$\max(\varepsilon) = \max\left(|\,\hat{\mathbb{W}} - W\,|\right),\ RMS = \sqrt{\frac{\sum_{i=1}^{N}\left(\hat{\mathbb{W}}_i - W_i\right)^2}{N}} \tag{8}$$

where W is the approximate solution and $\widehat{\mathbb{W}}$ is exact solution.

Example 1. The exact solution of the model (1) with $\beta = 1$, $\gamma = \delta = 0$:

$$W(\bar{r},t) = \mathrm{e}^{-t}\sin(\pi x)\sin(\pi y)\sin(\pi z),\ \ \bar{r} = (x,y,z) \in \Omega \tag{9}$$

where the source function can be adjusted according to the exact solution.

Table 1 show the results of *Example 1* for different values of α, t, $N = 20^3$, and $\tau = 0.0005$. In comparison with the method given in [11], it is observed tat thee results of the LMM are superior. Figure 1 visualized the comparison of exact and numerical solutions of the LMM for different values time-fractional order α with $N = 20^3$, $\tau = 0.0005$, and $t = 1$ and a good agreement has been found.

Numerical results for non-uniform nodes in non-rectangular domain are calculated in term of RMS and max(ε) at different time t which are visualized in fig. 1. It can be observed that the LMM can produced accurate results in case of non-rectangular domain.

Table 1. *Example 1*, results of the LMM

		$\alpha = 0.5$		$\alpha = 0.1$		
t	Method	max(ε)	*RMS*	max(ε)	*RMS*	Condition number
0.1	LMM	$1.800 \cdot 10^{-09}$	$6.145 \cdot 10^{-10}$	$1.800 \cdot 10^{-09}$	$6.145 \cdot 10^{-10}$	1.0000
	[11]	$1.885 \cdot 10^{-07}$	$5.777 \cdot 10^{-08}$	$1.885 \cdot 10^{-07}$	$5.777 \cdot 10^{-08}$	
0.4	LMM	$5.335 \cdot 10^{-09}$	$1.821 \cdot 10^{-09}$	$5.335 \cdot 10^{-09}$	$1.821 \cdot 10^{-09}$	1.0000
	[11]	$5.586 \cdot 10^{-07}$	$1.712 \cdot 10^{-07}$	$5.586 \cdot 10^{-07}$	$1.712 \cdot 10^{-07}$	
0.7	LMM	$6.916 \cdot 10^{-09}$	$2.361 \cdot 10^{-09}$	$6.916 \cdot 10^{-09}$	$2.361 \cdot 10^{-09}$	1.0000
	[11]	$7.242 \cdot 10^{-07}$	$2.219 \cdot 10^{-07}$	$7.242 \cdot 10^{-07}$	$2.219 \cdot 10^{-07}$	
	LMM	$7.320 \cdot 10^{-09}$	$2.498 \cdot 10^{-09}$	$7.320 \cdot 10^{-09}$	$2.498 \cdot 10^{-09}$	1.0000
	[11]	$7.664 \cdot 10^{-07}$	$2.349 \cdot 10^{-07}$	$7.664 \cdot 10^{-07}$	$2.349 \cdot 10^{-07}$	

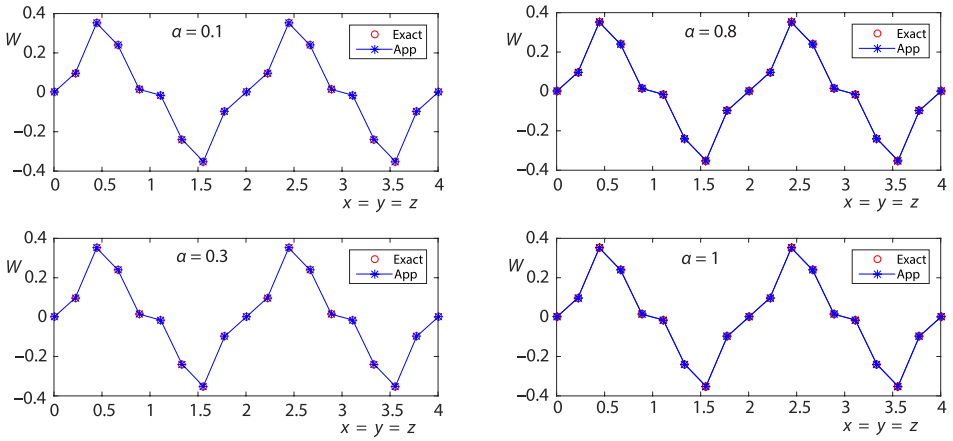

Figure 1. *Example 1*, numerical solution and exact solution at different α

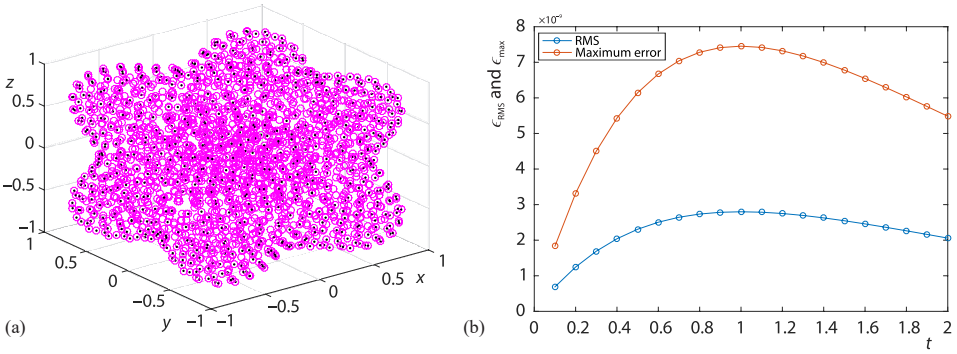

Figure 2. *Example 1*, (a) domain and (b) error in term of RMS max(ε)

Conclusion

In order to explore 3-D time-fractional Sobolev equations, we have employed a realistic numerical technique termed the local meshless algorithm based on radial basis functions. The problem is discretized in the time direction using the Crank-Nicolson time-integration method first, and then the local meshless method is applied. In comparison methods described in recent literature, the current method constructed a sparse linear system of equations with an ideal lower condition number and accurately approximated the solution.

Acknowledgment

Taif University Researchers Supporting Project No. (TURSP-2020/154), Taif University, Taif, Saudi Arabia.

References

[1] Diethelm, K., *The Analysis of Fractional Differential Equations: An Application-Oriented Exposition Using Differential Operators of Caputo Type*, Springer Science and Business Media, Berlin, Germany, 2010
[2] Caputo, M., Linear Models of Dissipation Whose Q is almost Frequency Independent-II, *Geophysical Journal International*, *13* (1967) 5, pp. 529-539
[3] Wang, F., *et al.*, Gaussian Radial Basis Functions Method for Linear and Non-Linear Convection-Diffusion Models in Physical Phenomena, *Open Physics*, *19* (2021), 1, pp. 69-76
[4] Wang, F., *et al*., Formation of Intermetallic Phases in Ion Implantation, *Journal of Mathematics*, *2020* (2020), ID8875976
[5] Nawaz, R., *et al*., An Extension of Optimal Auxiliary Function Method to Fractional Order High Dimensional Equations, *Alexandria Engineering Journal*, *60* (2021), 5, pp. 4809-4818
[6] Ahmad, I., et al., Application of Local Meshless Method for the Solution of Two Term Time Fractional-Order Multi-Dimensional PDE Arising in Heat and Mass Transfer, *Thermal Science*, *24* (2020), Suppl. 1, pp. 95-105
[7] Ahmad, I., *et al.*, Numerical Simulation of PDE by Local Meshless Differential Quadrature Collocation Method, *Symmetry*, *11* (2019) 3, 394
[8] Ahmad, I., *et al*., An Efficient Local Formulation for Time-Dependent PDE, *Mathematics*, *7* (2019), 216
[9] Ahmad, I., *et al*., Local RBF Method for Multi-Dimensional Partial Differential Equations, Computers *and Mathematics with Applications*, *74* (2017), 2, pp. 292-324
[10] Shu, C., *Differential Quadrature and Its Application in Engineering*, Springer-Verlag, London, UK, 2000
[11] Haq, S., Hussain, M., Application of Meshfree Spectral Method for the Solution of Multi-Dimensional Time-Fractional Sobolev Equations, *Engineering Analysis with Boundary Elements*, *106* (2019), Sept., pp. 201-216
[12] Ulutas, E., *et al*., Bright, Dark, and Singular Optical Soliton Solutions for Perturbed Gerdjikov-Ivanov Equation, *Thermal Science*, *25* (2021), Special Issue 2, pp. S151-S156
[13] Ulutas, E., *et al*., Exact Solutions of Stochastic KdV Equation with Conformable Derivatives in white Noise Environment, *Thermal Science*, *25* (2021), Special Issue 2, pp. S143-S149
[14] Yildirim, E. N., *et al.*, Reproducing Kernel Functions and Homogenizing Transforms, *Thermal Science*, *25* (2021), Special Issue 2, pp. S9-S18
[15] Abdelrahman, M. A. E., *et al.*, Exact Solutions of the Cubic Boussinesq and the Coupled Higgs Systems, *Thermal Science*, *24* (2020), Suppl. 1, pp. S333-S342
[16] Menni, Y., *et al.*, Heat and Mass Transfer of Oils in Baffled and Finned Ducts, *Thermal Science*, *24* (2021), Suppl. 1, pp. S267-S276

Paper submitted: August 20, 2022
Paper revised: September 28, 2022
Paper accepted: November 15, 2022